Turkish Journal of Physics

Volume 26 | Number 1 Article 1

1-1-2002

The Sensitivity of c\rightarrow u \gamma decay in the Gluino-Axion Model

MÜGE BOZ

Turk J Phys
26 (2002) , 1 – 11.

The Sensitivity of $c \to u\gamma$ decay in the Gluino-Axion Model*

Müge BOZ
Physics Department, Hacettepe University,
06532 Ankara-TURKEY

Received 25.05.2001

Abstract

The sensitivity of $c \to u\gamma$ decay in the recently proposed gluino-axion model is analyzed for a light sbottom in a restricted parameter space. The decay rate enhances up to 3% with respect to the SM result in a moderate range of $\tan\beta$ values.

1. Introduction

In the standard electroweak theory (SM) the single phase in the CKM matrix θ_{CKM} is a unique source for both flavour and CP violations. In the supersymmetric (SUSY) extensions of the standard model, there exist novel sources for both flavour and CP violations coming from the soft supersymmetry breaking mass terms [1]. The new sources of CP violation can be probed via the flavour conserving processes such as the Higgs system [2] and the electric dipole moments (EDM) [3] of the particles. On the other hand, a searching platform for flavour violation is the flavour–changing processes generally arising at one and higher loop orders [4,5,6].

It is now a well–known fact that mixing [7,8] and decays [9,10] of D mesons, as well as K and B meson processes [11] are very important tools in searching for the new physics effects via the loops of the new particles. In this work, our main interest will be the radiative charm decays. The radiative decay $D \to \pi\gamma$, which is represented by the radiative decay $c \to u\gamma$, at the parton level, has been analyzed using different methods and levels of precision [12,13]. In Ref. [14], the sensitivity of this decay is analyzed in detail in the context of minimal SUSY standard model (MSSM). In Ref. [15], the analysis of $c \to u\gamma$ has been also done in the same context, but in a restricted parameter space with the light scalar bottom quark [16,17]. For such $\Delta F = 1$ decays, the charginos contribute in a manner with no need for flavour-changing mixing [18]. Therefore, with the aim of saturating the existing EDM bounds, the sfermions of the first two generations are assumed to be heavy enough($\geq$ TeV) and approximately degenerate such that their contributions decouple for any loop of interest. Within such an approximation, it is clear that the contribution of the chargino-squark loops will be the only essential ones.

It has been observed in Ref. [16] that the light sbottom ($\tilde{b}_1$) could be as light as the bottom quark itself. Moreover, the corresponding parameter space favours the light stop to be degenerate with the top quark itself:

$$M_{\tilde{t}_1} = 175 \text{ GeV} \quad \text{and} \quad M_{\tilde{b}_1} = 5 \text{ GeV} \ . \tag{1}$$

The compatibility of a light bottom squark in the unconstrained MSSM has been recently studied in Ref. [17], where the renormalization group flow up to Grand Unification Scale is considered. Unlike Ref. [17], in

*This work was partially supported by the Turkish Scientific and Technical Research Council (TÜBİTAK) under the project, No:TBAG-2002(100T108).

Ref. [15] only chargino, charged Higgs and W-boson loops give contribution to the underlying model, whereas the gluino mass is not included. In this work, however, we will make our analysis in the recently proposed gluino-axion model [19,20].

The supersymmetric (SUSY) theories, which are designed to solve the hierarchy problems, possess two hierarchy problems: One concerning the strong CP problem, also existing in the S.M, whose source is the neutron EDM exceeding the present bounds by nine orders of magnitude and the other is the μ puzzle, concerning the Higgsino Dirac mass parameter μ, which follows from the superpotential of the model. A simultaneous solution to these two hierarchy problems is achieved in Ref. [19] in the context of supersymmetry with a new kind of axion [21,22] which couples to the gluino rather than to quarks. In the gluino-axion model the invariance of the SUSY Lagrangian and all supersymmetry breaking terms under $U(1)_R$ is guaranteed by promoting the ordinary μ parameter to a composite operator involving the gauge singlet $\hat{S}$ with unit R charge. When the scalar component of the singlet develops vacuum expectation value (VEV) around the Peccei–Quinn scale $\sim 10^{11}$ GeV, an effective μ parameter $\mu \sim$ aTeV is induced. Besides, the low energy theory is identical to minimal SUSY model with all sources of soft SUSY phases. Due to all these abilities of the model of Ref. [19], in solving the hierarchy problems, in the analysis below we will adopt its parameter space.

Assuming that all the sfermions of the first two generations are heavy enough to decouple and all generation changing entries of the sfermion mass matrices vanish, in what follows, we will analyze $\Gamma(c \to u\gamma)$ in units of the SM result. In doing this: (i) the Wilson coefficients are evolved down to the mesonic mass scale for a phenomenologically sensible description; (ii) all the supersymmetric contributions, as well as the the contributions of the charged Higgs and W-boson loops, are calculated at the weak scale; (iii) due to its restricted parameter space, we work in the gluino-axion model [19], where the soft masses needed for this analysis are expressed in terms of the μ parameter through appropriate flavour matrices

The organization of this work is as follows. In Sect. 2, starting from the low energy Lagrangian of the model, we define the soft masses which we need for this analysis. We work on the sbottom and chargino contributions in Sects 2.1 and 2.2. In Sec. 2.3, armed with full diagonalization of the squark and chargino sectors, we discuss the one-loop contributions to the Wilson coefficients. A numerical study of the theoretical predictions in comparison with that of the SM is performed in Sec. 3. We summarize our conclusions in Sec. 4.

2. The Model

In the gluino-axion model of Ref. [19], the soft terms of the low energy Lagrangian are identical to those in the general MSSM:

$$\begin{aligned}
\mathcal{L}^{soft}_{MSSM} &= \tilde{Q}^\dagger M^2_{\tilde{Q}} \tilde{Q} + \tilde{u^c}^\dagger M^2_{u^c} \tilde{u^c} + \tilde{d^c}^\dagger M^2_{d^c} \tilde{d^c} + \tilde{L}^\dagger M^2_{\tilde{L}} \tilde{L} \\
&+ \tilde{e^c}^\dagger M^2_{e^c} \tilde{e^c} + \Big\{ \big[A_u \tilde{Q} \cdot H_u \ \tilde{u^c} + A_d \tilde{Q} \cdot H_d \ \tilde{d^c} \\
&+ A_e \tilde{L} \cdot H_d \ \tilde{e^c} \big] + h.c. \Big\} + M^2_{H_u} |H_u|^2 \\
&+ M^2_{H_d} |H_d|^2 + (\mu \ B H_u \cdot H_d + h.c.) \\
&+ \Big\{ M_3 \tilde{\lambda}^a_3 \tilde{\lambda}^a_3 + M_2 \tilde{\lambda}^i_2 \tilde{\lambda}^i_2 + M_1 \tilde{\lambda}_1 \tilde{\lambda}_1 + h.c. \Big\},
\end{aligned} \tag{2}$$

except for the fact that the soft masses are proportional to the the μ parameter via appropriate flavour matrices. (Note that here, and in what follows, we will neglect the effects of axion, axino and saxino interactions as their couplings are severely suppressed [19].) The flavour matrices form the sources of CP violation and intergenerational mixings in the squark sector. The phases of the trilinear couplings ($A_{u,d,e}$), the gaugino masses ($M_{3,2,1}$), and the effective μ–parameter

$$\mu \equiv v_s^2 / M_{Pl} \times e^{-i\theta_{QCD}/3} \sim \text{a TeV} \times e^{-i\theta_{QCD}/3}, \tag{3}$$

are the only phases which contribute to CP violation observables. In this formula for μ parameter, $v_s \sim 10^{11}$ GeV is the Peccei–Quinn scale, and θ_{QCD} is the effective QCD vacuum angle. In the gluino-axion model

all the soft masses are expressed in terms of the μ parameter. In our analysis only the chargino and bottom squark loops contribute to the process, so that we will not need to express all the soft masses in terms of the μ parameter. Instead we will only need to specify the bottom squark soft masses, and the gaugino masses, namely:

(i) the bottom squark soft masses:

$$M^2_{\tilde{Q}} \;=\; k^2_Q\;|\mu|^2\;, \tag{4}$$

where k_Q is a real parameter;

(ii) the gaugino masses:

$$M_2 \;=\; k_2\;\mu\;, \tag{5}$$

where k_2 is a complex parameter.

2.1. Sbottom Sector

We start by analyzing the squark sector where the elements of the sbottom mass matrix $\widetilde{\mathcal{M}}^2_{b,ij}$ can be expressed in the weak basis $(\tilde{b}_L,\;\tilde{b}_R)$ as follows:

$$\widetilde{\mathcal{M}}^2_b \;=\; \begin{pmatrix} \tilde{M}^2_{b,11} & m_b(A_b-\mu\tan\beta) \\ m_b(A_b-\mu\tan\beta) & \tilde{M}^2_{b,22} \end{pmatrix}\;, \tag{6}$$

where

$$\begin{aligned} \tilde{M}^2_{b,11} &= k^2_Q\;|\mu|^2\;+\;m^2_b\;+\;\cos 2\beta M^2_Z\;(T^b_z\;-\;Q_b\sin^2\theta_w)\;, \\ \tilde{M}^2_{b,22} &= k^2_Q\;|\mu|^2\;+\;m^2_b\;+\;\cos 2\beta M^2_Z\;Q_b\sin^2\theta_w\;, \end{aligned} \tag{7}$$

with $Q_b=-1/3$, $T^b_z=-1/2$ and $\sin\theta_w=(1-M^2_W/M^2_Z)^{1/2}$. Moreover, the sbottom soft masses $M^2_{\tilde{Q}}$ are expressed in terms of the μ parameter(4). Additionally, the mass-squared eigenvalues are given by

$$\begin{aligned} M^2_{\tilde{b}_1(\tilde{b}_2)} &= \frac{1}{2}\Big\{2k^2_Q\;|\mu|^2+2m^2_b+T^b_z\cos 2\beta M^2_Z \\ &\quad -(+)\;\sqrt{\Big[\cos 2\beta M^2_Z(T^b_z-2Q_b\sin^2\theta_w)\Big]^2\;+\;4m^2_b(A_b-\mu R_b)^2}\;\Big\}. \end{aligned} \tag{8}$$

In the present scenario the light stop and sbottom masses are known, which allows one to solve one of the unknowns in (8) in terms of these known masses. We choose to solve the sbottom left–right entries $(A_b-\mu\tan\beta)$, that is:

$$\begin{aligned} (A_b-\mu\tan\beta) &= \frac{1}{m^2_b}\Big[\Big(M^2_{\tilde{b}_1}-k^2_Q\;|\mu|^2-m^2_b-(1/2)\;T^b_z\cos 2\beta M^2_Z\Big)^2 \\ &\quad -\;\frac{1}{4}\Big(\cos 2\beta M^2_Z(T^b_z-2Q_b\sin^2\theta_w)\Big)^2\Big]\;. \end{aligned} \tag{9}$$

One notes that the LR mixing parameter depends only on the sbottom soft mass $\tilde{M}^2_Q$ which is proportional to the μ parameter (4). As usual, the sbottom matrix $\widetilde{\mathcal{M}}^2_b$ can be diagonalized via the unitary rotation:

$$\begin{pmatrix} \tilde{b}_L \\ \tilde{b}_R \end{pmatrix} \;=\; \begin{pmatrix} \cos\theta_b & \sin\theta_b \\ -\sin\theta_b & \cos\theta_b \end{pmatrix}\cdot\begin{pmatrix} \tilde{b}_1 \\ \tilde{b}_2 \end{pmatrix}\;, \tag{10}$$

which relates the weak basis $(\tilde{b}_L,\;\tilde{b}_R)$ to the mass eigenstates $(\tilde{b}_1,\;\tilde{b}_2)$, whereas the mixing angle θ_b is defined as

$$\cos\theta_b \;=\; \frac{m_b(A_b-\tan\beta\mu)}{\sqrt{m^2_b(A_b-\tan\beta\mu)^2\;+\;\tilde{M}^2_{b,11}-M^2_{\tilde{b}_1}}}\;, \tag{11}$$

where $\tilde{M}^2_{b,11}$ is the 11–matrix element of $\widetilde{\mathcal{M}}^2_b$ defined in (7), $M^2_{\tilde{b}_1}$ is given by (8), and the numerator and the denominator of (11) are expressed in terms of (9).

2.2. Chargino Sector

We start with the 2×2 mass matrix [23] of the charginos which are the mass eigenstates of charged gauginos and Higgsinos:

$$M_C = \begin{pmatrix} k_2\mu & -\sqrt{2}M_W \cos\beta \\ -\sqrt{2}M_W \sin\beta & \mu \end{pmatrix} , \tag{12}$$

where the gaugino masses M_2 are expressed in terms of the μ parameter (5). The mass matrix of the charginos (12) can be diagonalized via the biunitary transformation:

$$C_R^\dagger M_C C_L = \mathrm{diag}(m_{\chi_1}, m_{\chi_2}) , \tag{13}$$

where C_L and C_R are 2×2 unitary matrices and m_{χ_1}, m_{χ_2} are the masses of the charginos χ_1, χ_2 such that $m_{\chi_1} > m_{\chi_2}$. For convinience, the following explicit parametrization can be chosen for the chargino mixing matrices:

$$C_{L(R)} \;=\; \begin{pmatrix} \cos\theta_{L(R)} & \sin\theta_{L(R)} \\ -\sin\theta_{L(R)} & \cos\theta_{L(R)} \end{pmatrix} , \tag{14}$$

where the angle parameters $\theta_{L(R)}$ can be determined from 13. After a straightforward calculation, one gets:

$$\tan 2\theta_{L(R)} \;=\; \frac{\sqrt{8}M_W \sqrt{k_2^2\ \mu^2 \cos^2\beta + \mu^2 \sin^2\beta + \mu^2 k_2 \sin 2\beta}}{k_2^2\ \mu^2 - \mu^2 - (+)2M_W^2 \cos 2\beta} , \tag{15}$$

and finally, the masses of the charginos are given by

$$\begin{aligned} m^2_{\chi_{1(2)}} \;&=\; \frac{1}{2}\Big\{k_2^2\ \mu^2 + \mu^2 + 2M_W^2 + (-)[(k_2^2\ \mu^2 - \mu^2)^2 + 4M_W^2 \cos^2 2\beta \\ &+\; 4M_W^2(k_2^2\ \mu^2 + \mu^2 + 2k_2\ \mu^2 \sin 2\beta)]^{1/2}\Big\}. \end{aligned} \tag{16}$$

Following the full diagonalization of the sbottom and the chargino sectors, in what follows, we will start working on the contributions to the Wilson coefficients from the chargino, charged Higgs and W-boson loops. Between these three types of contributions, the first one is of SUSY origin in which chargino and sbottom loops contribute while the other two are of S.M.

2.3. One Loop Contributions to The Wilson Coefficients

Analysis of the $c \to u\gamma$ decay follows closely that of the $b \to s\gamma$ decay [11,24]. The effective Hamiltonian, describing a $\Delta F = 1$ transition, is defined at the scale $\mu = M_W$ with the standard quark operators

$$H_{eff} = -\frac{G_F}{\sqrt{2}} \sum_{i=1}^{8} C_i \mathcal{O}_i , \tag{17}$$

where $\mathcal{O}_{i=1,\cdots,8}$ are the standard quark operators [25]. For a phenomenologically sensible description, the Wilson coefficients C_i are evolved down to the mesonic mass scale and, in solving the the Wilson coefficients, two successive steps are followed: first the Wilson coefficients are evolved from $\mu = M_W$ down to $\mu = m_b$ level using five active quark flavors, then these coefficients are run down to $\mu = m_c$ level for four active quark flavours. The details of this analysis, at $m = m_c$ level, are studied in Ref. [15]. However, we summarize our calculational procedure in Appendix A for completeness.

As all other radiative flavour–changing decays, $c \to u\gamma$ decay is described in terms of the coefficient C_7 evaluated at $\mu = m_c$:

$$\begin{aligned} C_7(m_c) &= C_7^{(0)}(m_c) + C_2(M_W)C_7^{(2)}(m_c) + C_7(M_W)C_7^{(7)}(m_c) \\ &\quad + C_8(M_W)C_7^{(8)}(m_c). \end{aligned} \tag{18}$$

The explicit expressions of each term in (18) are defined in Appendix A. One notes that $C_7(m_c)$ depends on three Wilson coefficients: $C_2(M_W)$, $C_7(M_W)$ and $C_8(M_W)$ and the determination of these short-distance coefficients reflects the properties of the model under consideration. Here, $C_2(M_W) = 1$, and $C_7(M_W)$ and $C_8(M_W)$ can be expressed as follows:

$$C_{7(8)}(M_W) = C_{7(8)}^{\chi}(M_W) + C_{7(8)}^{H^\pm}(M_W) + C_{7(8)}^{W}(M_W). \tag{19}$$

Clearly, these coefficients receive contributions from chargino, charged Higgs and W-boson loops. $C_{7(8)}^{\chi}(M_W)$ is the pure supersymmetric contribution, where chargino ($\chi^\pm$) and bottom squark ($\tilde{b}$) loops contribute to the process. $C_{7(8)}^{H^\pm}(M_W)$ and $C_{7(8)}^{W}(M_W)$ are the charged Higgs, and W–boson loop contributions respectively. The chargino contribution to $C_{7(8)}(M_W)$ can be expressed as

$$\begin{aligned} C_{7(8)}^{\chi}(M_W) &= \sum_{i=1}^{2}\sum_{k=1}^{2} \frac{M_W^2}{m_{\chi_i}^2}\frac{m_{\chi_i}^2}{M_{\tilde{b}_k}^2}\left[C_{L1i}S_{b1k} + \frac{h_b}{g_2}C_{L2i}S_{b2k}\right] \\ &\quad \left[\left(C_{L1i}S_{b1k} + \frac{h_b}{g_2}C_{L2i}S_{b2k}\right)K_1^{7(8)}(r_{ki}) - \right. \\ &\quad \left. \frac{h_t}{g_2}\frac{m_{\chi_i}}{m_t}C_{R2i}S_{b1k}K_2^{7(8)}(r_{ki})\right], \end{aligned} \tag{20}$$

where

$$\begin{aligned} h_t &= \frac{m_t g_2}{\sqrt{2}M_W \sin\beta}, \\ h_b &= \frac{m_b g_2}{\sqrt{2}M_W \cos\beta}, \end{aligned} \tag{21}$$

and

$$r_{ki} = \frac{m_{\chi_i}^2}{M_{\tilde{b}_k}^2}. \tag{22}$$

The contributions of charged Higgs bosons are given by:

$$C_{7(8)}^{H^\pm}(M_W) = -\frac{1}{2}r_h\left[\bar{K}_1^{7(8)}(r_H) + \tan^2\beta\bar{K}_2^{7(8)}(r_H)\right], \tag{23}$$

where

$$r_H = \frac{m_b^2}{M_{H^\pm}^2}. \tag{24}$$

Finally, the standard W-boson contributions lead to

$$C_{7(8)}^{W}(M_W) = -3\ r_W\bar{K}_1^{7(8)}(r_W), \tag{25}$$

where

$$r_W = \frac{m_b^2}{M_W^2}. \tag{26}$$

The loop functions $K_1^{7(8)}$ (20), (23) and $\bar{K}_1^{7(8)}$ (25) are defined in Appendix B.

Table 1. The maximum values of $\mathcal{R}_i(\%)$ for different k_2 and k_Q in a moderate range of $\tan\beta$ values. One notes that, for $\tan\beta = 4$, μ starts from 95 GeV whereas for $\tan\beta = 10$ and $\tan\beta = 15$, the lowest bounds of μ are 88 GeV and 87 GeV respectively.

$\tan\beta$	k_2	k_Q	μ_1	$\mathcal{R}_1(\%)$	μ_2	$\mathcal{R}_2(\%)$	μ_3	$\mathcal{R}_3(\%)$
4	2.5	1	95 GeV	2.431	88 GeV		87 GeV	
4	2.5	1.25	95 GeV	2.261	88 GeV		87 GeV	
4	2.5	1.5	95 GeV	1.863	88 GeV		87 GeV	
4	2.5	1.75	95 GeV	1.470	88 GeV		87 GeV	
4	2.5	2	95 GeV	1.125	88 GeV		87 GeV	
10	2.5	1	95 GeV	1.723	88 GeV	2.557	87 GeV	
10	2.5	1.25	95 GeV	1.815	88 GeV	2.662	87 GeV	
10	2.5	1.5	95 GeV	1.647	88 GeV	2.460	87 GeV	
10	2.5	1.75	95 GeV	1.394	88 GeV	2.099	87 GeV	
10	2.5	2	95 GeV	1.133	88 GeV	1.724	87 GeV	
15	2.5	1	95 GeV	1.240	88 GeV	1.869	87 GeV	2.031
15	2.5	1.25	95 GeV	1.393	88 GeV	1.905	87 GeV	2.032
15	2.5	1.5	95 GeV	1.371	88 GeV	1.939	87 GeV	2.082
15	2.5	1.75	95 GeV	1.207	88 GeV	1.731	87 GeV	1.860
15	2.5	2	95 GeV	0.997	88 GeV	1.456	87 GeV	1.567

3. Numerical Analysis

As mentioned in the Introduction, we analyze $c \to u\gamma$ decay in the light of recent experimental data, which requires $M_{\tilde{t}_1} = 175$ GeV and $M_{\tilde{b}_1} = 5$ GeV so that in the present scenario, light sbottom and the stop masses are known, allowing one to solve the LR mixing entry (9) in terms of the known masses.

A convinient way to observe the new physics effects is via the dimensionless quantity defined by

$$\mathcal{R} = \frac{\Gamma(c \to u\gamma)_{MSSM}}{\Gamma(c \to u\gamma)_{SM}} - 1, \tag{27}$$

which measures the fractional enhancement or suppression in the decay rate with respect to the SM value. One notes that $\mathcal{R}$ has been based on real parameters, namely real gaugino mass and the μ parameter. The phases of these parameters are very important in determining the CP asymetry of the decay. However, since the CP asymetry of this decay has not been measured yet, and only for the numerical analysis of $\mathcal{R}$, the parameters k_2 and μ are taken as real.

Using the formulae in the previous section, we will now perform a numerical study of $\mathcal{R}$ in the allowed range of the μ parameter and analyze the variation of this quantity with the positive and negative values of μ. As a reflecting property of the underlying model all the soft masses are expressed in terms of the μ parameter. Since the μ parameter is stabilized to the weak scale, as a consequence of the naturalness, all dimensionless parameters are expected to be $\mathcal{O}(1)$. Therefore, we take the dimensionless quantities k_2 and k_Q in $\mathcal{O}(1)$ and let $|\mu|$ vary from $|250|$ GeV to $|80|$ GeV. Moreover, we will study in a moderate range of $\tan\beta$ values, namely, $\tan\beta = 4$, $\tan\beta = 10$, $\tan\beta = 15$, $\tan\beta = 20$ to illustrate the variation of $\mathcal{R}$ with the μ parameter, for different values of k_2 and k_Q. Depicted in Table 1 is the variation of $\mathcal{R}(\%)$ for $\mu > 0$ with different values of k_2 and k_Q. One notes that the allowed range of the μ parameter, and so as the lowest value of μ, depends on $\tan\beta$ as well as the the other parameters of the model under consideration. For instance, for $\tan\beta = 4$, the lowest bound of μ starts from 95 GeV, whereas for $\tan\beta = 10$ the bound is lowered to 88 GeV and for $\tan\beta = 15$, to 87 GeV. Although not shown in the table, the starting value of μ for $\tan\beta = 20$ is 86 GeV.

It is observed that for the cases $k_2 = 1$ and $k_Q = 1$ and $k_2 = 1.5$ and $k_Q = 1.5$, there are no solutions for $\mathcal{R}(\%)$ since in both cases chargino masses are imaginary. The solutions for $\mathcal{R}(\%)$ start only when $k_2 = 2$,

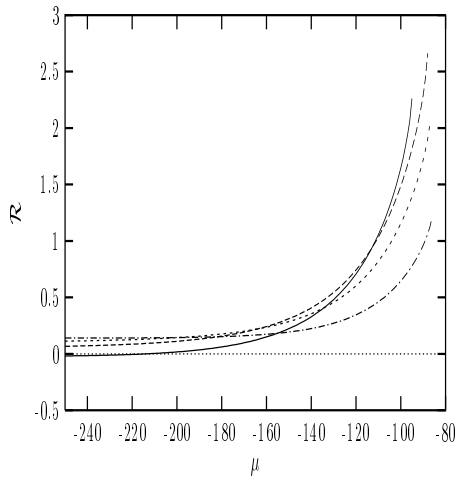

Figure 1. Variation of $\mathcal{R}(\%)$ with $\mu < 0$ for $\tan\beta = 4$ (solid curve), $\tan\beta = 10$ (dashed curve), $\tan\beta = 15$(dotted curve), $\tan\beta = 20$ (dot-dashed curve) with $k_2 = 2.5$ and $k_Q = 1.25$.

but for convinience, we summarize the data starting from $k_2 = 2.5$ for different values of k_Q in Table 1. It is also noticable that for values of k_2 larger than 3, the data for $\mathcal{R}(\%)$ are not favorable.

In Fig. 1, the variation of $\mathcal{R}(\%)$ is shown for $\mu < 0$, with four different values of $\tan\beta = 4$ (solid curve), $\tan\beta = 10$ (dashed curve), $\tan\beta = 15$ (dotted–curve) and $\tan\beta = 20$ (dot–dashed curve). In between the different values of k_2 and k_Q, we concentrate on one particular $k_2, k_Q s$ pair and make our analysis for the case where $k_2 = 2.5$ and $k_Q = 1.25$. Moreover, since $\mathcal{R}(\%)$ remains constant at about $\sim 0.1\%$ in the range between -500 GeV to -250 GeV, we discard this region of the parameter space which does not make sense for our analysis. Instead, we concentrate on the interval as μ ranges from -250 GeV to -80 GeV. One notes that as μ increases, the supersymmetric contribution decreases in accordance with the decoupling of the supersymmetric contribution.

As the figure suggests, for $\tan\beta = 10$ (dashed curve) $\mathcal{R}$ increases from $\sim 0.2\%$ up to $\sim 3\%$ level, and for $\tan\beta = 4$ (solid curve) it increases up to $\sim 2.5\%$ level as μ ranges from -250 GeV to -80 GeV. Though the behaviour is similar, for larger $\tan\beta$, $\mathcal{R}$ decreases faster. Indeed it can be at most $\sim 2\%$ for $\tan\beta = 15$ and $\sim 1.25\%$ for $\tan\beta = 20$. It is observed in this analysis that for larger $\tan\beta$ values, $\tan\beta > 20$, the enhancement in the rate remains always below 1%, thereby leaving a small window of observation.

As is noted immediately from the figure, although the maximum value of $\mathcal{R}(\%)$ decreases with increasing $\tan\beta$, the maximum value of $\mathcal{R}(\%)$ for $\tan\beta = 10$ is greater than the one for $\tan\beta = 4$. This effect can be easily understood by observing the dependency of $\tan\beta$ on the lowest value of μ as noted before. (The maximum value of $\mathcal{R}$ is 2.7 for 88 GeV, it decreases to 1.8 at 95 GeV for $\tan\beta = 10$, whereas for $\tan\beta = 4$, its value at 95 GeV is 2.4 but for 88 GeV there is no solution).

Fig. 2 is similar to Fig. 1, except for the choice of positive μ parameter. Being an approximate mirror of Fig. 1, $\mathcal{R}$ again decreases with increasing μ.

From the analysis of these two figures showing the variation of $\mathcal{R}(\%)$ in a moderate range of $\tan\beta$ values, in general, one can arrive at a conclusion that theoretically, this region is favorite since the enhancement is more than 1% for most of the parameter space, that is, $b \to s\gamma$ decay is as well in the allowed band of CLEO data.

4. Conclusions

In this work, we have analyzed $c \to u\gamma$ decay in the gluino-axion model for a light scalar bottom quark. The scalar bottom quark enters the chargino contribution, and thus, influences the decay rate. For

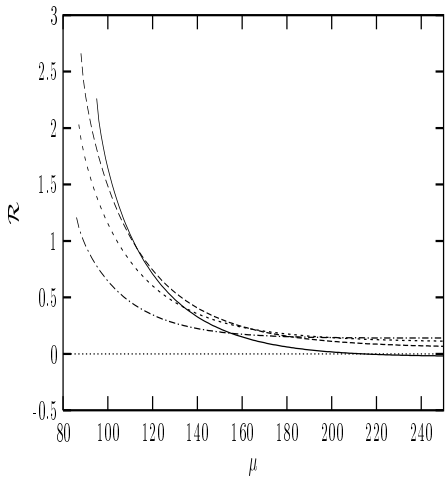

Figure 2. The same as Fig. 1 but $\mu > 0$.

a moderate range of $\tan\beta$ values (where there is no danger of violating the CLEO result on $b \to s\gamma$ decay rate), we find that the rate is enhanced up to $\sim 3\%$ with respect to the SM.

Before closing, we would like to point out that:

- Although the numerical analysis of the branching ratio based on real parameters, namely real gaugino mass and the μ parameter, in general the phases of these parameters are crucial for determining the CP asymetry of the decay. The phases of these parameters contribute to direct CP violation as well as $D^0 - \bar{D}^0$ mixing as in the Kaon and B-meson systems. However, the CP asymetry of this decay has not been measured yet, so the complex parameters are not analyzed in this work.

- Besides such direct measurements, another important clue for CP violation in charm-quark systems (e.g D-meson) is the formation of P-wave charmoniums; especially the phases of the trilinear couplings, the A-parameters defined in (2), can be directly probed by the observation of such CP odd charmonium levels at lepton colliders [26]. Moreover, it is known that the A-parameters are never constrained by any other observable such as the Higgs system and EDMs.

Acknowledgements

The author thanks D. A. Demir for useful conversations.

References

[1] M. Dugan, B. Grinstein and L. Hall, *Nucl. Phys.* **B255**, (1985) 413.

[2] A. Pilaftsis, *Phys. Lett.,* **B435** (1998) 88 [hep-ph/9805373]; D. A. Demir, *Phys. Rev.,* **D60** (1999) 055006 [hep-ph/9901389]; A. Pilaftsis and C. E. Wagner, *Nucl. Phys.,* **B553** (1999) 3 [hep-ph/9902371]; M. Carena, J. Ellis, A. Pilaftsis and C. E. Wagner, *Nucl. Phys.,* **B586** (2000) 92 [hep-ph/0003180]; S. Y. Choi, M. Drees and J. S. Lee, *Phys. Lett.,* **B481** (2000) 57 [hep-ph/0002287]; T. Ibrahim and P. Nath, *Phys. Rev.,* **D63**, 035009 (2001) [hep-ph/0008237].

[3] P. Nath, *Phys. Rev. Lett.,* **66** (1991) 2565; Y. Kizukuri and N. Oshimo, *Phys. Rev.,* **D45** (1992) 1806; T. Ibrahim and P. Nath, *Phys. Lett.,* **B418** (1998) 98 [hep-ph/9707409]; S. Pokorski, J. Rosiek and C. A. Savoy, *Nucl. Phys.,* **B570** (2000) 81 [hep-ph/9906206].

[4] Y. Nir, [hep-ph/9810520].

[5] H. E. Haber and G. L. Kane, *Phys. Rept.,* **117** (1985) 75.

[6] M. Misiak, S. Pokorski and J. Rosiek, [hep-ph/9703442].

[7] G. C. Branco, P. A. Parada and M. N. Rebelo, *Phys. Rev.,* **D52** (1995) 4217 [hep-ph/9501347].

[8] A. F. Falk, Y. Nir and A. A. Petrov, *JHEP,* **9912** (1999) 019 [hep-ph/9911369].

[9] C. Grab, *SLAC-PUB-4372, Invite Talk given at Int. Europhysics Conf. on High Energy Physics, Uppsala, Sweden, Jun 25- Jul 1, 1987.*

[10] I. Bigi, F. Gabbiani and A. Masiero, *Z. Phys.,* **C48** (1990) 633.

[11] F. Bertolini, F. Borzumati, A. Masiero and G. Ridolfi, *Nucl. Phys.,* **B353** (1991) 591.

[12] S. Fajfer and P. Singer, *Phys. Rev.* **D56** (1997) 4302 [hep-ph/9705327]; B. Bajc, S. Fajfer and R. J. Oakes, *Phys. Rev.* **D54** (1996) 5883 [hep-ph/9509361]; S. Fajfer, S. Prelovsek and P. Singer, *Phys. Rev. D* **59** (1999) 114003 [hep-ph/9901252].

[13] C. Greub, T. Hurth, M. Misiak and D. Wyler, *Phys. Lett.* **B382** (1996) 415 [hep-ph/9603417].

[14] S. Prelovsek and D. Wyler, *Phys. Lett.* **B500** (2001) 304 [hep-ph/0012116].

[15] M. Boz and Z. Kırca, *Mod. Phys. Lett.,* **A15** (2001) 2345.

[16] M. Carena, S. Heinemeyer, C. E. Wagner and G. Weiglein, [hep-ph/0008023].

[17] A. Dedes and H. K. Dreiner, [hep-ph/0009001].

[18] D. A. Demir, A. Masiero and O. Vives, *Phys. Rev. Lett.,* **82** (1999) 2447 [hep-ph/9812337].

[19] D. A. Demir, E. Ma, *Phys. Rev.,* **D62** (2000) 111901 [hep-ph/0004148].

[20] D. A. Demir, E. Ma and U. Sarkar, *J. Phys.,* **G26** (2000) L117 [hep-ph/0005288]. D. A. Demir and E. Ma, [hep-ph/0101185].

[21] R. D. Peccei and H. R. Quinn, *Phys. Rev. Lett.,* **38** (1977) 1440.

[22] J. E. Kim, *Phys. Rev. Lett.,* **43** (1979) 103; M. A. Shifman, A. I. Vainshtein and V. I. Zakharov, *Nucl. Phys.,* **B166** (1980) 493; M. Dine, W. Fischler and M. Srednicki, *Phys. Lett.,* **B104** (1981) 199.

[23] D. A. Demir *Phys. Rev.,* **D60** (1999) 095007 [hep-ph/9905571].

[24] M. Aoki, G. Cho and N. Oshimo, *Nucl. Phys.,* **B554** (1999) 50 [hep-ph/9903385]; *Phys. Rev.,* **D60** (1999) 035004 [hep-ph/9811251];

[25] A. J. Buras, M. Misiak, M. Munz and S. Pokorski, *Nucl. Phys.,* **B424** (1994) 374 [hep-ph/9311345].

[26] D. A. Demir and M. B. Voloshin, Phys. Rev. D **63** (2001) 115011 [hep-ph/0012123].

[27] G. Burdman, E. Golowich, J. L. Hewett and S. Pakvasa, *Phys. Rev.,* **D52** (1995) 6383 [hep-ph/9502329].

Appendix A

The solutions of the QCD renormalization group equations (RGE) can be expressed as:

$$C_k(\mu) = U_{kl}^{5(4)}(\mu, M_W) C_l(M_W), \tag{28}$$

where U_{kl}^5 and U_{kl}^4 are the evaluation matrices defined in five and four flavour contexts, respectively, and can be determined by the following expressions [27]:

$$\begin{aligned} U^5(m_b, M_W)_{kn} &= O_{kl} \left[\eta_b^{\vec{a_l}}\right] O_{kn}^{-1} , \\ \eta_b &= \frac{\alpha_s(M_W)}{\alpha_s(m_b)} , \\ U^4(m_c, m_b)_{kn} &= O_{kl} \left[\eta_{bc}^{\vec{a_l}}\right] O_{kn}^{-1} , \\ \eta_{bc} &= \frac{\alpha_s(m_b)}{\alpha_s(m_c)} . \end{aligned} \tag{29}$$

In the above expression, $\vec{a_l} \equiv \frac{\gamma_{ll}^D}{2\beta_0}$ with $\beta_0 = \frac{11-2n_f}{3}$, in which f can be taken as 4(5) as needed, and $\gamma^D = O^{-1}\gamma^{(eff)T}O$ is the diagonalized 8×8 anamolous dimension matrix.

The explicit expressions for each term in (18) can be obtained after the solution of (29):

$$C_7^{(0)}(m_c) = \sum_{i=1}^{8} \eta_b^{a_i} f_i(\eta_{bc}) , \tag{30}$$

where the numbers a_i are given by

$$a_i = \Big(0.609 \ , \ 0.696 \ , \ -0.423 \ , \ 0.261 \ , \ 0.146 \ , \ -0.522 \ , \ -0.899 \ , \ 0.409 \ \Big) , \tag{31}$$

and

$$\begin{aligned} f_1(\eta_{bc}) &= 2.2996 \ \eta_{bc}^{0.640} , \quad f_2(\eta_{bc}) = -1.09 \ \eta_{bc}^{0.640} , \\ f_3(\eta_{bc}) &= -0.001 \ \eta_{bc}^{-0.845} + 0.027 \ \eta_{bc}^{-0.420} - 0.0004 \ \eta_{bc}^{0.132} \\ &\quad -0.032 \ \eta_{bc}^{0.347} + 0.483 \ \eta_{bc}^{0.560} - 0.516 \ \eta_{bc}^{0.640} , \\ f_4(\eta_{bc}) &= 0.0002 \ \eta_{bc}^{-0.845} - 0.0006 \ \eta_{bc}^{-0.420} - 0.0010 \ \eta_{bc}^{0.132} \\ &\quad +0.4 \ \eta_{bc}^{0.240} + 0.107 \ \eta_{bc}^{0.347} - 0.546 \ \eta_{bc}^{0.560} - 0.388 \ \eta_{bc}^{0.640} , \\ f_5(\eta_{bc}) &= +0.00004 \ \eta_{bc}^{-0.845} - 0.00009 \ \eta_{bc}^{-0.42} - 0.0057 \ \eta_{bc}^{0.132} \\ &\quad +0.006 \ \eta_{bc}^{0.347} + 0.084 \ \eta_{bc}^{0.560} - 0.091 \ \eta_{bc}^{0.640} , \\ f_6(\eta_{bc}) &= +0.017 \ \eta_{bc}^{-0.845} + 0.016 \ \eta_{bc}^{-0.420} + 0.00042 \ \eta_{bc}^{0.132} \\ &\quad +0.032 \ \eta_{bc}^{0.347} - 0.084 \ \eta_{bc}^{0.560} - 0.038 \ \eta_{bc}^{0.640} , \\ f_7(\eta_{bc}) &= 0.0065 \ \eta_{bc}^{-0.845} + 0.00044 \ \eta_c^{-0.420} + 0.00006 \ \eta_{bc}^{0.132} \\ &\quad +0.004 \ \eta_{bc}^{0.347} - 0.267 \ \eta_{bc}^{0.560} + 0.238 \ \eta_{bc}^{0.640} , \\ f_8(\eta_{bc}) &= -0.0004 \ \eta_{bc}^{-0.845} + 0.00096 \ \eta_{bc}^{-0.420} + 0.0008 \ \eta_{bc}^{0.132} \\ &\quad +0.728 \ \eta_{bc}^{0.347} - 3.744 \ \eta_{bc}^{0.560} + 2.365 \ \eta_{bc}^{0.640} . \end{aligned} \tag{32}$$

The second term $C_7^{(2)}(m_c)$ is given by

$$C_7^{(2)}(m_c) = \sum_{i=1}^{2} \eta_{bc}^{r_i} g_i(\eta_b) , \tag{33}$$

and the numbers r_i read as

$$r_i = \Big(0.560 \ , \ 0.640\Big) , \tag{34}$$

and

$$\begin{aligned} g_1(\eta_b) &= 0.304\ \eta_b^{-0.899} - 0.466\ \eta_b^{-0.423} - 0.111\ \eta_b^{0.146} \\ &\quad +4.872\ \eta_b^{0.409} - 4.599\ \eta_b^{0.609}\ , \\ g_2(\eta_b) &= -0.304\ \eta_b^{-0.899} + 0.466\ \eta_b^{-0.423} + 0.111\ \eta_b^{0.146}\ , \\ &\quad -4.872\ \eta_b^{0.409} + 4.599\ \eta_b^{0.609}\ . \end{aligned} \tag{35}$$

For the third term, $C_7^{(7)}(m_c)$, in (18) we find

$$C_7^{(7)}(m_c) = C_7(M_W)\eta_b^{0.696}\eta_{bc}^{0.640}\ . \tag{36}$$

Finally, $C_7^{(8)}(m_c)$ in (18) is given by:

$$C_7^{(8)}(m_c) = C_8(M_W)\sum_{i=1}^{2}\eta_{bc}^{s_i}h_i(\eta_b)\ , \tag{37}$$

where

$$s_i = \Big(0.560\ ,\ 0.640\Big)\ , \tag{38}$$

and

$$\begin{aligned} h_1(\eta_b) &= -5.333\ \eta_b^{0.609}\ , \\ h_2(\eta_b) &= 2.667\ \eta_b^{0.609} + 5.333\ \eta_b^{0.609} - 2.667\ \eta_b^{0.696}\ . \end{aligned} \tag{39}$$

Appendix B

The loop functions $K_1^7(r)$ and $K_2^7(r)$ are defined as:

$$\begin{aligned} K_{1(2)}^7(r) &= I_{1(2)}(r) - \frac{1}{3}J_{1(2)}(r)\ , \\ K_{1(2)}^8(r) &= J_{1(2)}(r)\ . \end{aligned} \tag{40}$$

where the functions $I_1(r)$, $I_1(r)$ and $J_1(r)$, $J_2(r)$, can be expressed as:

$$\begin{aligned} I_1(r) &= \frac{1}{12(1-r)^4}(2+3r-6r^2+r^3+6r\ln r)\ , \\ I_2(r) &= \frac{1}{12(1-r)^3}(-3+4r-r^2-2\ln r), \\ J_1(r) &= \frac{1}{12(1-r)^4}(1-6r+3r^2+2r^3-6r^2\ln r), \\ J_2(r) &= \frac{1}{12(1-r)^3}(1-r^2+2r\ln r)\ . \end{aligned} \tag{41}$$

$$\begin{aligned} \bar{K}_{1(2)}^7(r) &= J_{1(2)}(r) - \frac{1}{3}I_{1(2)}(r)\ , \\ \bar{K}_{1(2)}^8(r) &= I_{1(2)}(r)\ . \end{aligned} \tag{42}$$